BIOCHEMISTRY
including biophysical chemistry & molecular biology
Article

Biochemistry **2010,** *49,* 1207–1216 1207
DOI: 10.1021/bi9017208

Decoding of Lipoprotein−Receptor Interactions: Properties of Ligand Binding Modules Governing Interactions with Apolipoprotein E[†]

Miklos Guttman, J. Helena Prieto, Johnny E. Croy, and Elizabeth A. Komives*

Department of Chemistry and Biochemistry, University of California, San Diego, 9500 Gilman Drive, La Jolla, California 92093-0378

Received October 7, 2009; Revised Manuscript Received December 22, 2009

ABSTRACT: Clusters of complement-type ligand binding repeats in the LDL receptor family are thought to mediate the interactions between these receptors and their various ligands. Apolipoprotein E, a key ligand for cholesterol homeostasis, has been shown to interact with LDLR, LRP, and VLDLR, through these clusters. LDLR and VLDLR each contain a single ligand binding repeat cluster, whereas LRP contains three large clusters of ligand binding repeats, each with ligand binding functions. We show that within sLRP3 the three-repeat subcluster CR16−18 recapitulated ligand binding to the isolated receptor binding portion of ApoE (residues 130−149). Binding experiments with LA3−5 of LDLR and CR16−18 showed that a conserved W25/D30 pair appears to be critical for high-affinity binding to ApoE(130−149). The triple repeat LA3−5 showed the expected interaction with ApoE(1−191)·DMPC, but surprisingly CR16−18 did not interact with this form of ApoE. To understand these differences in ApoE binding affinity, we introduced mutations of conserved residues from LA5 into CR18 and produced a CR16−18 variant capable of binding ApoE-(1−191)·DMPC. This change cannot fully be accounted for by the interaction with the proposed ApoE receptor binding region; therefore, we speculate that LA5 is recognizing a distinct epitope on ApoE that may only exist in the lipid-bound form. The combination of avidity effects with this distinct recognition process likely governs the ApoE−LDL receptor interaction.

The low-density lipoprotein (LDL) superfamily of receptors mediates cholesterol uptake into cells (*1*). Members of this family share many structural characteristics and sequence homology including an extracellular ligand binding domain consisting of complement-type repeats (CRs),[1] also called ligand binding modules (LAs), epidermal growth factor precursor homology repeats (EGFs), β-propeller domains, and a single transmembrane segment with an intracellular domain (Figure 1). The most well characterized of these receptors, LDLR, is genetically linked to hypercholesterolemia (*2*). LDLR family members recognize apolipoproteins on the surface of lipid particles, and apolipoprotein E, in particular, plays an important role in receptor-mediated cholesterol uptake (*3*). Although LDLR is the primary receptor for cholesterol-carrying lipoproteins, studies have shown that the LDL receptor-related protein (LRP) and the very low density lipoprotein receptor (VLDL) also mediate the uptake of ApoE-enriched β-VLDLs (*4*−*7*).

LRP recognizes at least 30 different ligands which indicate the diversity of LRP's functions (*8*). The 600 kDa precursor is processed by furin cleavage, and the two chains remain noncovalently bound at the cell surface (*9*). The receptor-associated protein (RAP) serves as a chaperone assisting the maturation of LRP (*10*, *11*) and can interact with ligand binding clusters of this family of receptors, blocking the binding of certain ligands (*12*). Each of the three helical bundle domains of RAP can interact with receptors, but the third domain (RAPD3) has the highest affinity for these ligand binding clusters (*13*). A semi-conserved aspartate within these CRs was shown to be critical for RAP binding (*14*). The extracellular chain of LRP contains four clusters of CRs referred to as sLRPs (Figure 1). Studies have shown that isolated sLRPs can interact with many ligands of LRP *in vitro* (*15*−*18*). Much like LDLR, LRP was shown to bind and internalize β-VLDLs, but only if the VLDLs were enriched with ApoE (*4*). Other distinctions between the two receptors have been observed including calcium dependence (*19*, *20*) and RAP inhibition of ligand binding (*12*, *18*).

Each CR/LA domain is composed of about 40 amino acids with a well-conserved fold stabilized by three disulfide bonds and a cluster of acidic residues that form a high-affinity calcium binding site. Mutations at the calcium binding site wreck proper folding and are associated with familial hypercholesterolemia (*21*). Several CR domains have now been solved by both NMR and crystallographic methods (*22*) and show very little deviation in their overall fold. It is believed that high variability in short loops of these repeats results in different surface contours and electrostatics, which establish ligand specificity (*1*, *23*).

ApoE is a constituent of several lipoprotein particles, and common alleles have been associated with type III hyperlipoproteinemia (*24*). ApoE is composed of two domains that are both involved in lipid binding, but only the N-terminal domain is

[†]This work was supported by NIH Grant AG025343.

*To whom correspondence should be addressed. Phone: (858) 534-3058. Fax: (858) 534-6174. E-mail: ekomives@ucsd.edu.

[1]Abbreviations: ApoE, apolipoprotein E; CR, complement-type repeat and ligand binding repeat of LRP; DMPC, dimyristoylphosphatidylcholine; EDTA, ethylenediaminetetraacetic acid; GST-RAP, glutathione *S*-transferase fused receptor associated protein; HMW, high molecular weight; HPLC, high-performance liquid chromatography; HSQC, heteronuclear single-quantum coherence; LA, ligand binding repeat of LDLR; LDLR, low-density lipoprotein receptor; LRP, LDL receptor-related protein; PCR, polymerase chain reaction; sLRP, ligand binding cluster of LRP; VLA, ligand binding repeat of VLDLR; VLDLR, very low density lipoprotein receptor.

Published on Web 12/23/2009

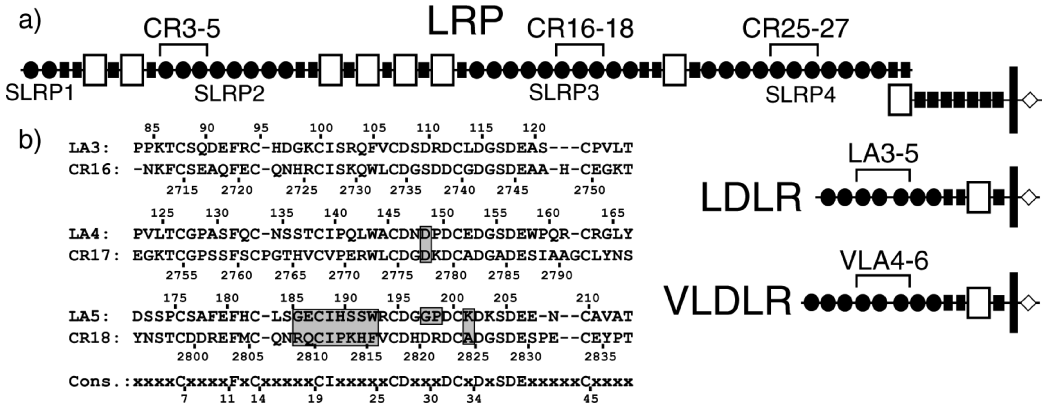

FIGURE 1: (a) Schematic diagram of LRP, LDL, and VLDL showing CR/LA modules (circles), EGF domains (black rectangles), β-propeller domains (clear rectangles), and intracellular domain (diamonds). (b) Sequence alignment of LA3−5 with CR16−18 with overall consensus for complement repeats (*21*). Highlighted portions were mutated in this study, including the β2-swap mutation inserting residues 186−193 of LA5 into CR18 at positions 2809−2816.

required for receptor binding (*25*). Several studies agree that the critical receptor recognition site is within residues 140−150 (*26*−*28*). Chimeric lipoproteins in which this segment is spliced into an unrelated lipoprotein have found that substitution with residues 131−151 of ApoE is enough for receptor recognition (*29*). Peptides from this region of ApoE incorporated into lipoprotein particles enhanced uptake both *in vitro* and *in vivo* (*30*, *31*). Binding studies with ApoE(130−149) and ApoE(140−151)[2] have shown that both can directly interact with the three complete sLRPs (2, 3, and 4) of LRP (*32*).

The structure of the N-terminal domain of ApoE has been solved (*33*), and although residues 131−151 form a surface-accessible helix in the structure, the N-terminal domain alone cannot bind LDL receptors with high affinity. Low-resolution structural information indicates that the ApoE helical bundle adopts a new conformation when it is present in lipoprotein particles (*34*−*36*). Our hypothesis is that when embedded in lipoprotein particles, ApoE residues 140−150 are in a different conformation for high-affinity receptor binding than that observed in the crystal structure of the N-terminal domain alone (*37*). In addition, upon lipid binding, the region downstream of the 140−150 site, which also contains critical residues for receptor binding, becomes structured (*24*, *38*−*40*). Thus, it is also possible that this downstream region forms a high-affinity receptor recognition site in the lipid-bound state of ApoE.

Studies aimed at narrowing down the exact binding modules involved in recognizing ApoE have found minimal units in LDLR (*41*, *42*) and VLDLR (*43*), but similar studies on LRP have not yet been performed. Deletion studies in LDLR have implicated LA5 as the critical repeat for β-VLDL binding (*42*). LA45 was shown to be the minimal unit of LDLR capable of binding ApoE(1−191)·dimyristoylphosphatidylcholine (DMPC) particles *in vitro*, which mimic the lipid-bound conformer of ApoE (*41*). Similar studies have implicated repeats 5 and 6 (VLA56) of VLDLR in ApoE binding (*43*). Interestingly, both LA45 and VLA56 have a uniquely long linker sequence connecting the two repeats. On the basis of these data we performed sequence alignments in order to discover possible ApoE binding sites in LRP. We present results from binding experiments on a three-CR repeat fragment of LRP and comparisons of its binding with combinations of repeats from LDLR. Together, the results reveal specific regions within LDLRs that govern the mechanism by which they recognize ApoE-containing lipoproteins.

MATERIALS AND METHODS

Sequence Alignments. Sequence alignments were performed to search for the three-CR repeat sequences that would most likely bind to ApoE based on the fact that within LDLR the three-repeat segment LA3−5 contains the ApoE binding site. The LA3−5 sequence (Uniprot number P01130) (residues 84−214, numbering referring to the mature protein) without the additional linker between LA4 and LA5 (residues 167−172) was used to search for homology within each sLRP (Uniprot number Q07954), using sequence alignment with LALIGN software (Bill Pearson, University of Virginia, Charlottesville) with the BLOSUM35 matrix with default values entered for gap penalty. The regions that contained the highest homology in each sLRP were CR3−5 (831−956), CR16−18 (2712−2838), and CR25−27 (3471−3516) (numbering according to mature LRP-1). To further analyze the sequences for unique residues that might be involved in ApoE binding, alignments of LA45 from LDLR and VLA56 from VLDLR from various species were made with genedoc 2.6 (*44*) (Uniprot numbers P01130, P98155, P35951, P98156, P35952, P98166, Q28832, P35950, Q99087, Q6NS01, Q99088, O77505, P20063, P35953, P98165, Q7ZZT0, and Q6S4M2).

Protein Expression and Purification. Smaller subdomains of LRP, CR3−5, CR16−18, and CR25−27, were cloned into the pPIC9K as described previously for thrombomodulin (*45*). CR16 (2712−2754), CR17 (2751−2798), CR18 (2794−2838), and multiple repeats CR16−17, CR17−18, and CR16−18 of human LRP and residues 88−126 (LA3), 123−167 (LA4), 171−214 (LA5), 123−214 (LA4−5), and 88−235 (LA3−5) of the human LDLR (numbering for mature forms) were amplified by PCR and cloned into the pMMHb vector (*46*) modified to include an additional thrombin cleavage site after the TrpLE peptide. DNA oligonucleotides were inserted at the 3′ *Bam*HI site to yield a C-terminal FLAG tag. All mutants were made using either inverse PCR (*47*) or QuickChange (Stratagene, La Jolla, CA) mutagenesis and verified by DNA sequencing. CR17[3] was constructed by inserting CR17 with identical sticky ends into the *Bam*HI site of CR17 in the pMMHb vector and screening for multiple insertions with correct orientation. Inverse PCR mutagenesis was used to remove CR17 from CR16−18 yielding a two-repeat CR16(Δ17)18. A β2-swap mutation was made in CR18 in which residues 186−193 of LA5 were substituted into CR18 at positions 2809−2816. An expression vector for His-tagged ApoE(1−191) was a kind gift from S. Blacklow. A ubiquitin

(Ub) fusion vector was generated by cloning the DNA sequence for human ubiquitin into the *Nco*I and *Bam*HI sites of vector pHis8 (*48*). RAPD3(218−323) and ApoE(130−149) were inserted at the 3′ end of this ubiquitin (Ub) fusion vector to generate Ub-RAPD3 and Ub-ApoE(130−149). ApoE(130−149) and ApoE(141−155)^2 were synthesized with N-terminal biotinylation on a 9050 peptide synthesizer (Applied Biosystems, Foster City, CA). A scrambled ApoE(130−149) was also synthesized with the sequence LREKKLRVSALRTHRLELRL. Purification of GST-RAP has been described previously (*18*). His-tagged ApoE-(1−191) was expressed in BL21-DE3, purified, and complexed with dimyristoylphosphatidylcholine (DMPC) (Avanti Polar Lipids, Alabaster, AL) as described previously (*41*). Ub-ApoE(130−149) was expressed and purified as described for Ub-RAPD3, with an additional cation-exchange step prior to gel filtration to remove degradation products (Guttman et al., submitted).

LRP sLRPs were expressed in *Pichia pastoris* as described previously (*18*). Each CR fragment was expressed in *Escherichia coli* strain BL21-DE3 cells. Cultures were grown in M9 minimal media supplemented with NZ amine at 37 °C to OD_{600} 1.0 and induced with 0.5 mM IPTG. Isotopic labeling was achieved using M9 minimal media with $^{15}NH_4Cl$ (1 g/L) and [^{13}C]glucose (3 g/L) (Cambridge Isotope Laboratories, Andover, MA). After 12 h of expression, cells were harvested and lysed by sonication. Inclusion bodies were isolated by centrifugation and resuspended in resolubilizing buffer (8 M urea, 50 mM Tris (pH 8.0), 150 mM NaCl, 1 mM β-mercaptoethanol). Proteins were captured with Ni-NTA (Qiagen, Hilden, Germany) and washed with a gradient (50−50 mL) of resolubilizing buffer to refolding buffer (50 mM Tris (pH 8.2), 400 mM NaCl, 10 mM $CaCl_2$, and 1.5 mM/0.4 mM reduced/oxidized glutathione). Columns were sealed, and the resin was allowed to mix continuously by rocking in refolding buffer at 4 °C for 3 days after which they were washed with 50 mM Tris (pH 8.0), 150 mM NaCl, and 10 mM $CaCl_2$ and treated with active bovine thrombin (40 μg/L of expressed protein) for 12 h at 25 °C. Refolded, cleaved CRs were then purified by C18 reverse-phase HPLC (Waters, Milford, MA). Constructs containing LA4 needed an additional purification step to resolve disulfide isomers (Guttman et al., submitted). The purified CR repeats(s) were lyophilized from the HPLC buffer and stored at −80 °C. All expressed proteins were analyzed by MALDI-TOF on a Voyager DE-STR (Applied Biosystems, Foster City, CA) with sinnapinic acid (Agilent, Santa Clara, CA) as the matrix.

Biacore. SPR experiments were performed on a Biacore3000 with 300 RUs of biotinylated ApoE(130−149) or ApoE-(141−155)^2 immobilized onto the chip (*32*). Binding sensorgrams were collected for a series of sLRP subdomains ranging in concentration from 62.5 nM to 16 μM at 5 μL/min. The surface was regenerated between injections by a 2 min injection of 1 M NaCl. Each series of injections was fit globally to a 1:1 binding model with a drifting baseline using BiaEvaluation v.3.1.

ITC. Calcium binding to various CR and LA repeats was assessed by titrations monitored with a MicroCal VP-ITC calorimeter. Lyophilized protein was resuspended in 20 mM Hepes (pH 7.4), 150 mM NaCl, and 0.02% azide that was treated with Chelex (Bio-Rad, Hercules, CA). CR and LA repeats were titrated with a 10-fold molar excess of $CaCl_2$ in the same buffer at 35 °C. Binding isotherms were fit to single binding site models in Origin 6.0, except CR16−18 which was fit to a two-site binding model (OriginLab, Northampton, MA).

ApoE(130−149) Pull Downs. All reactions were carried out in HBST (20 mM Hepes, pH 7.4, 150 mM NaCl, 0.02% sodium azide, 0.1% Tween-20 (Bio-Rad, Hercules, CA) containing either 2 mM $CaCl_2$ or 2 mM EDTA. ApoE(130−149) peptide with an N-terminal biotin was immobilized onto streptavidin agarose (Fluka, Buchs, Switzerland) at saturating concentrations as described previously (*32*). Either uncoupled beads or scrambled ApoE(130−149) peptide was used as a negative control. FLAG-tagged complement repeat constructs were added (500 nM), and reactions were left rocking at 25 °C for 2 h, then washed twice with the same buffer, resolved by SDS−PAGE, probed with anti-FLAG rabbit serum (a generous gift from P. van der Geer), and detected by chemiluminescence (Western Lightening Plus kit, Perkin-Elmer, Waltham, MA). GST-RAP (6 μM) and high molecular weight (HMW) heparin (5 mg/mL) (Sigma-Aldrich, St. Louis, MO) were tested as inhibitors. For comparisons of CR16−18, CR16−17, CR17−18, and CR16(Δ17)18, 500 nM and 5 μM concentrations were used in similar pull-down binding assays.

GST-RAP and ApoE·DMPC Pull Downs. GST-RAP (1 μM) or ApoE(1−191)·DMPC (2 μM) was mixed with various FLAG-tagged LA/CR constructs (1 μM), at 25 °C for 1 h, in HBST with either 1 mM calcium or 1 mM EDTA. In order to avoid the high background caused by minor precipitation of ApoE·DMPC, reactions were centrifuged for 5 min after the incubation step, and the supernatant was added to anti-FLAG agarose (Sigma-Aldrich, St. Louis, MO) for 30 min. Pull downs were washed three times in binding buffer, resolved by SDS−PAGE, and probed by Western blot with antibodies anti-ApoE (Millipore, Billerica, MA), anti-GST (GE Healthcare, Uppsala, Sweden), and anti-FLAG rabbit serum. RAP competition was performed with addition of 6 μM (3-fold excess) of GST-RAP.

NMR. NMR spectra were collected on a Bruker Avance 800 MHz or a Bruker Avance III 600 MHz spectrometer equipped with a cryoprobe at 307 K. ^{15}N,^{13}C-labeled CR16−18 (0.5 mM) was resuspended in 20 mM Hepes (pH 6.6), 150 mM NaCl, 5 mM $CaCl_2$, 50 mM arginine, 50 mM glutamic acid, 10% D_2O, and 0.02% sodium azide. Amide assignments were made with ^{1}H−^{15}N HSQC, HNCO, HNCA, HN(CO)CA, and HNCACB experiments. Assignments for CR17 were also made using a 0.7 mM sample of ^{15}N,^{13}C-labeled CR17 at pH 7.45 in the same buffer, with HSQC, CBCANH, and CBCANNH experiments. ^{15}N-labeled CR16 (0.4 mM) and CR18 (0.6 mM) were titrated from pH 6.6 to pH 7.45 to monitor pH-dependent chemical shift changes and to transfer the assignments from CR16−18 at pH 6.6. ^{15}N,^{13}C-labeled LA45 was assigned with the same experiments and buffer conditions used for CR17, except without 50 mM Arg/Glu, and assignments were transferred to individual LA4 and LA5. The data were processed using Azara (Wayne Boucher and the Department of Biochemistry, University of Cambridge) and analyzed in Sparky (T. D. Goddard and D. G. Kneller, SPARKY 3, University of California, San Francisco). All assignment data for CR16−18, CR17, and LA45 have been deposited to the BMRB (IDs 16509, 16482, and16480).

NMR Titrations. All titrations of CR/LA(s) with various ligands were performed in 20 mM Hepes (pH 7.45), 150 mM NaCl, 10 mM $CaCl_2$, and 0.02% azide in 10% D_2O at 307 K. Due to self-association of CR17, all CR concentrations were kept under 100 μM, which became problematic at large excess of titrated ligands due to the appearance of peaks from natural abundance ^{15}N from the ligand. Identical aliquots of ^{15}N-labeled CR/LAs were resuspended in either Ub-fused ligand or Ub,

adjusted to pH 7.45, and mixed in various ratios to yield samples with varying concentrations of ligand but identical total protein concentration. Only well-resolved peaks in all titrations were used for affinity calculations. Some residues exhibited slow exchange binding kinetics in the CR18-RAPD3 titrations, so only shifts showing fast exchange kinetics were analyzed. For some titrations the highest ligand concentration could not be included in the fit due to poor signal-to-noise ratio and broadening of peaks. ^{15}N shifts were normalized by a factor of 9.8, and the net shift for every cross-peak in both ^{1}H and ^{15}N was calculated. A global fit of all perturbations (> 0.015 ppm) was implemented as described previously (*49*). Titration curves were also fit to measurements of the largest cross-peak perturbation and the sum of the absolute values of all individual perturbations. Overall K_Ds are reported as the average from these three methods, with the standard deviation of all measurements.

RESULTS

Identification of an ApoE Binding Subdomain in sLRP3. Alignments of each sLRP in LRP1 with LA3−5 in LDLR showed that CR3−5, CR16−18, and CR25−27 had the highest similarity to LA3−5. These subdomains were cloned and expressed in *P. pastoris* for surface plasmon resonance (SPR) analysis. Experiments to probe the binding of each sLRP subdomain to immobilized biotinylated ApoE(141−155)^2 and biotinylated ApoE(130−149) showed that, of the three, only CR16−18 had binding affinities comparable to the full-length sLRP (K_D ~200 nM) (Supporting Information Figure 1). SPR experiments also revealed that CR16−18 refolded from *E. coli* inclusion bodies bound as well as when purified from *P. pastoris*. Affinity pull-down assays verified that CR16−18 could bind immobilized ApoE(130−149) and that this interaction was calcium dependent and inhibited by heparin and RAP (Figure 2a). Pull-down assays of FLAG-tagged CR constructs also showed that two repeat constructs had significantly weaker affinity for ApoE(130−149), of which CR1718 bound the best (Figure 2b). CR17−18 also exhibited roughly 10-fold weaker binding as qualitatively assessed by SPR analysis.

Refolding and Calcium Binding of the LRP1 CR(s). Refolded LRP1 CR(s) were titrated with calcium, and binding was monitored by isothermal titration calorimetry (ITC). Calcium affinities for CR16, CR17, and CR18, were 0.72 ± 0.04 μM, 7.5 ± 2 μM, and 13.7 ± 0.7 μM, respectively, which are similar to previously published values for CR/LA domains (*50*, *51*). Calcium titration of the three repeat CR16−18 showed two binding events, and the data were fit to a two-site binding model (Figure 3a). Although the first site has relatively few data points, the thermodynamic parameters are consistent with CR16 binding initially with high affinity, followed by CR17 and CR18 binding with weaker affinity but higher enthalpy. Mutation of D2778 to Ala in CR17 had no effect on calcium affinity (K_D 7.4 ± 0.5 μM). NMR ^{1}H−^{15}N HSQC spectra in the presence of calcium indicated that each repeat was well folded, both as the isolated domain and in the CR16−18 subdomain (Figure 3b). Nearly all of the expected cross-peaks were observed for CR16 and CR18, but a significant number (12 of 49) of cross-peaks in CR17 were missing.

Titrations of ApoE(130−149) Binding to LRP1 CR(s). NMR titrations were used to examine the binding of CR16−18 to ApoE(130−149). Initial titration experiments with ApoE(130−149) peptide resulted in solubility problems, so ApoE(130−149) was expressed as a ubiquitin (Ub) fusion protein, and

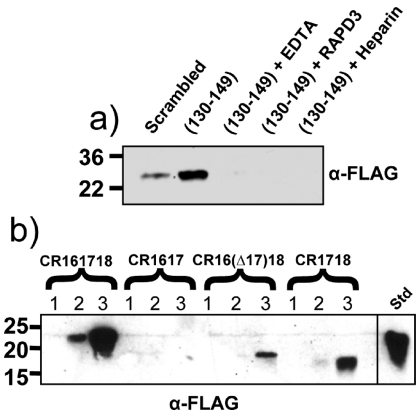

FIGURE 2: (a) FLAG-tagged CR16−18 was tested for binding to a scrambled ApoE peptide and ApoE(130−149) (both biotinylated and bound to streptavidin beads) in the presence of EDTA, RAP, and HMW heparin. The bound CR16−18 was visualized by anti-FLAG immunoblotting. (b) Same affinity assay as in (a) comparing smaller double repeats from CR16−18 with (1) 2.0 μM CR domain and unconjugated beads, (2) 100 nM CR domain and immobilized ApoE(130−149), or (3) 2.0 μM CR domain and immobilized ApoE-(130−149).

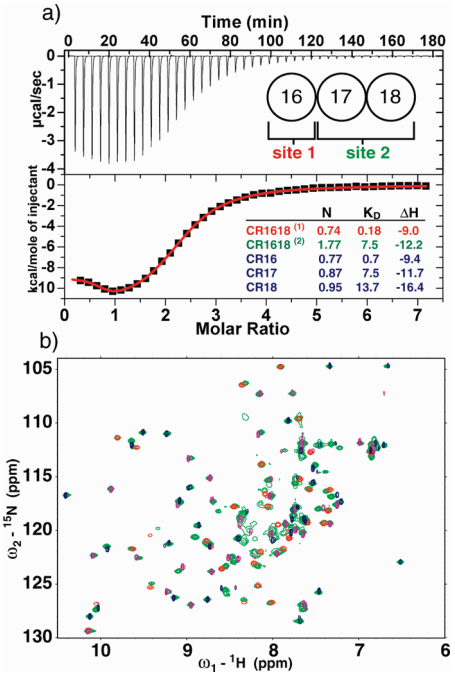

FIGURE 3: (a) Calcium binding isotherm of CR16−18. The inset provides values for the stoichiometry (N), the K_D (μM), and the ΔH (kcal/mol) are listed for each isolated CR (blue font) as well as for the fits of site 1 (red font) and site 2 (green font) in CR16−18. (b) NMR HSQC spectral overlays of CR16 (blue), CR17 (red), CR18 (purple), and CR16−18 (green) under identical conditions.

this alleviated the solubility problems even at concentrations above 1 mM. Binding of Ub-ApoE(130−149) caused specific perturbations in each repeat (Supporting Information Figure 2). The most notable perturbation was a strong downfield ^{1}H shift for the indole of W2773 in CR17. The same was true for the indoles of W2732 in CR16 and W144 in LA4. F2816, which is in the same position in CR18, showed the largest perturbation in this repeat. Other amides showing large perturbations included the following: K2730, W2732, D2735, G2736, S2737, and A2746 in CR16; F2760, C2768, V2769, R2772, W2773, D2776, and A2790 in CR17; R2809, C2818, D2829, and E2833 in CR18;

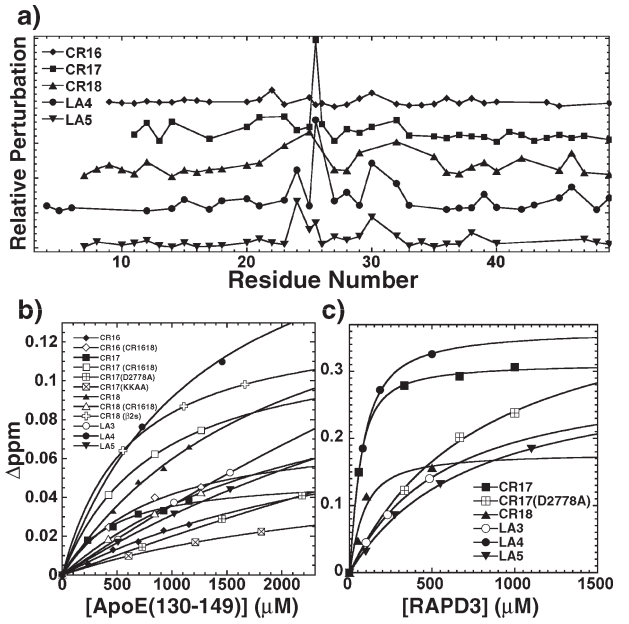

FIGURE 4: (a) Plot of relative amide perturbation for each residue in CR16 (◆), CR17 (■), CR18 (▲), LA4 (●), and LA5 (▼). CRs are each renumbered for alignments shown in Figure 1b, and indole side chains of W25 are plotted at the *x*-axis value of 25.5. (b) NMR titrations plots for Ub-ApoE(130−149) with CR16 (◆), CR16 in CR16−18 (◇), CR17 (■), CR17 in CR16−18 (□), CR17(D2778A) (+), CR17 with ApoE(130−149) (K143/146A) (×), CR18 (▲), CR18 in CR16−18 (Δ), CR18(*β*2swap) (open cross), LA3 (○), LA4 (●), and LA5 (▼). (c) NMR titrations for Ub-RAPD3 with the same symbols from (b). For both plots the largest resolvable amide perturbation was plotted against the ligand concentration.

W144, D147, D149, and D151 in LA4; and S172, W173, and G178 in LA5. Titrations of Ub-ApoE(130−149) with individual CRs showed shifts identical to those observed in CR16−18 (Supporting Information Figure 3). Plots of relative perturbations in each show the majority of large shifts are located in two loops between the third and fifth cysteines (residues 23−32 according to consensus numbering in Figure 1), but there was also significant variability of which residues shifted more among the three repeats (Figure 4a). Some amide cross-peaks which were nearly invisible in CR17 (C2762, C2768) became well resolved upon addition of ApoE(130−149), hinting that slow dynamics in apo CR17 are reduced in the ApoE(130−149)-bound form.

Due to the weak binding and small shifts, three different fitting methods were implemented to calculate K_Ds from these titrations, giving remarkably similar results for most cases (Table 1). These calculations revealed that CR17 had the highest affinity for ApoE(130−149) both isolated (930 μM) and in the context of CR16−18 (650 μM), similar to values for LA4 (1.1 mM) from the LDLR (Table 1, Figure 4b). CR18 had a weaker affinity (1.6 mM) both alone and in the context of CR16−18. CR16 had a very weak affinity as an isolated repeat (3.2 mM) but a strong affinity in the context of CR16−18 (733 μM). LA5 and especially LA3 showed a very weak affinity (3.9 mM and >5 mM, respectively) for ApoE(130−149).

To ensure the observed affinity was purely the result of the interaction with ApoE(130−149), CR17 was also titrated with two variants of ApoE: Ub-ApoE(130−149)(K143/146A) and Ub-ApoE(130−140). These titrations showed that the double mutation of the critical lysines, K143 and K146, to alanines significantly weakened binding (3.5 mM), and truncation of the last nine residues (ApoE(130−140)) nearly abolished it

Table 1: Binding Affinities for Various ApoE-LA/CR Interactions

	K_D (global)	K_D (largest)	K_D (sum)	K_D (overall)
		Ub-RAPD3 Binding		
CR17	33 ± 8	33 ± 3	40 ± 6	35 ± 4
CR17(D2778A)	710 ± 62	770 ± 130	680 ± 95	720 ± 46
CR18	55 ± 5	57 ± 30	62 ± 33	58 ± 4
LA3	460 ± 22	530 ± 4	480 ± 40	490 ± 36
LA4	52 ± 5	50 ± 2	46 ± 4	49 ± 3
LA5	650 ± 35	700 ± 70	660 ± 52	670 ± 26
		Ub-ApoE(130−149) Binding		
CR16	ND[a]	3176 ± 1050	ND	3176 ± ND
CR17	1027 ± 284	852 ± 334	912 ± 205	930 ± 89
CR17 (D2778A)	3496 ± 729	ND	3545 ± 250	3521 ± 35
CR18	1441 ± 266	1975 ± 381	1349 ± 163	1588 ± 338
CR18 (*β*2swap)	756 ± 61	560 ± 3	920 ± 77	745 ± 180
CR16 (in CR16−18)	774 ± 102	744 ± 183	681 ± 67	733 ± 47
CR17 (in CR16−18)	581 ± 92	757 ± 7	610 ± 19	649 ± 94
CR18 (in CR16−18)	1194 ± 239	2249 ± 220	1289 ± 90	1577 ± 584
LA3	8509 ± 3018	ND	9961 ± 160	9235 ± 1027
LA4	1031 ± 73	1197 ± 106	1049 ± 26	1092 ± 91
LA5	3822 ± 433	4189 ± 538	3622 ± 167	3878 ± 288
		Ub-ApoE(130−149) (K143/146A) Binding		
CR17	3840 ± 801	2761 ± 361	3776 ± 375	3459 ± 605
		Ub-ApoE(130−140) Binding		
CR17	ND	ND	ND	>5 mM

[a]ND: certain titrations could not be fit or yielded K_D values >5 mM with large uncertainty.

(>5 mM). Similarly, mutation of D2778 in CR17 (D2778A), that has been shown to be important for RAP binding, decreased the affinity for ApoE(130−149) significantly (3.5 mM) (*14*).

The results from titrations of the LRP CRs with ApoE-(130−149) indicated that individual CRs could each bind ApoE-(130−149). To see whether RAP might elicit similar chemical shift perturbations in the CRs, we titrated the individual CRs with RAPD3. Although two CRs are known to be required for high-affinity binding of RAPD3 (*14*), strong chemical shift perturbations were observed with single CRs (Supporting Information Figure 4). In CR17 and LA4 the largest perturbation was a downfield ^{1}H shift for the indole of W2773 and W144, exactly as seen with ApoE(130−149). The overall pattern of shifted residues was similar to that from ApoE(130−149) binding, with notable differences in the direction of shifts for R2772, W2773, and D2778. The C2781 amide also showed a large perturbation, and the cross-peaks for C2762 and C2768, which were weak in CR17, became stronger upon ApoE(130−149) binding but disappeared upon RAPD3 binding. Cross-peaks in CR18 showed both fast and slow exchange kinetics when perturbed by RAPD3 binding. C2806, N2808, D2821, and D2823 showed the largest perturbations with fast exchange, of which D2823 shifted in the same direction as upon ApoE-(130−149) binding (Supporting Information Figures 2 and 4). Cross-peaks for D2800, D2812, K2814, and F2816 could not be followed due to the slow kinetics of exchange. The fast

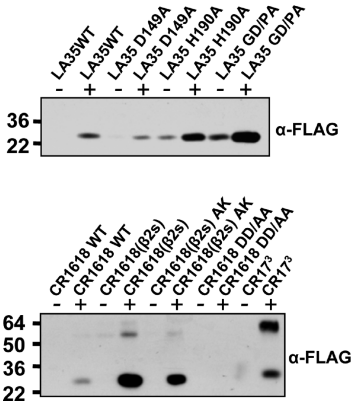

FIGURE 5: Affinity pull downs of various LA/CR constructs to scrambled peptide (−) or ApoE(130−149) (+), visualized by anti-FLAG immunoblotting. LA35 GD/PA refers to G198D/P199A, CR1618(β2s) refers to the β2swap mutant, AK is the A2825K mutation in CR18(β2swap), and CR1618 DDAA is the D2778A/D2821A double mutant.

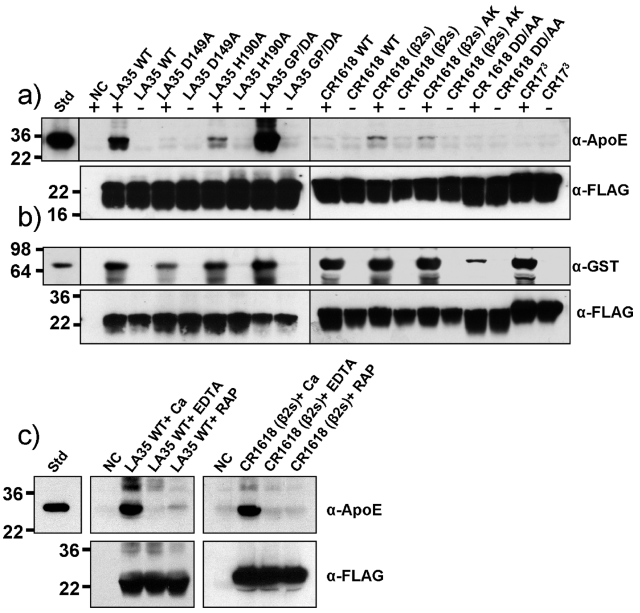

FIGURE 6: (a) Various LA/CR constructs and mutants were assayed for binding ApoE(1−191)·DMPC particles in the presence of calcium (+) or EDTA (−). Blots were visualized by anti-ApoE (top) and anti-FLAG (bottom) immunoblotting. (b) Same CR/LA constructs assayed for GST-RAP binding, visualized by α-GST (top) and anti-FLAG (bottom) immunoblotting. LA35 GD/PA refers to G198D/P199A, CR1618(β2s) refers to the β2swap mutant, AK is the A2825K mutation in CR18(β2swap), and CR1618 DDAA is the D2778A/D2821A double mutant. (c) Binding assays of LA3−5 and CR16−18(β2s) binding ApoE(1−191)·DMPC and inhibition with EDTA and GST-RAP.

exchanging chemical shift perturbations were fit to titration curves in the same manner as was done for ApoE (Table 1). Each of the individual CRs bound RAPD3 roughly 10-fold tighter than ApoE(130−149). CR17, CR18, and LA4 had the strongest affinities (35, 58, and 49 μM, respectively) (Table 1, Figure 4c). LA3 and LA5 had a much weaker affinities (490 and 670 μM), and the mutation of the critical Asp in CR17 (D2778A) again showed a drastic decrease in K_D for RAPD3 (720 μM).

Binding to ApoE(1−191)·DMPC. To examine the interaction with the full receptor binding site of lipid-complexed ApoE, Flag-tagged LA3−5 and CR16−18 were used for pull-down assays with ApoE(1−191)·DMPC. As expected, both constructs could interact with GST-RAP in a calcium-dependent manner (*41*), but only LA3−5 showed binding to ApoE(1−191)·DMPC. This was a surprising result considering that CR16−18 bound ApoE(130−149) with similar properties and was discovered by sequence similarity to LA3−5. To test whether multiple copies of a CR with high ApoE(130−149) affinity could interact with lipid-complexed ApoE, a triple CR17 ($CR17^3$) was constructed. Despite a strong interaction with ApoE(130−149) and GST-RAP, $CR17^3$ showed no interaction with ApoE(1−191)·DMPC (Figures 5 and 6).

D149 in LA4, D2778 in CR17, and D2821 in CR18 (all equivalent to D30 in the consensus) showed chemical shift perturbation upon RAPD3 binding in NMR titrations, and mutation of this residue in CR17 disrupted binding of ApoE(130−149) and RAPD3 (see above). We mutated each of these to Ala in LA3−5 and CR16−18 to test for effects on ApoE(1−191)·DMPC binding. Mutation of D149A(D30A) in LA4 weakened binding to ApoE(130−149) and GST-RAP and completely abolished ApoE(1−191)·DMPC binding (Figures 5 and 6). Similarly, alanine mutation of the critical D2778 and D2821(both D30) in CR17 and CR18 dramatically weakened GST-RAP binding and abolished ApoE(130−149) binding. Just like wild type, this double mutant also did not bind ApoE(1−191)·DMPC.

LA5, which bound ApoE(130−149) weakly, has a Gly at position 30 instead of an Asp. To test the importance of this site further, we mutated G198D(G30D) and P199A(P31A) in LA5 to introduce this missing Asp. Surprisingly, this substitution in LA5 dramatically enhanced both ApoE(130−149) and calcium-dependent ApoE(1−191)·DMPC binding (Figures 5 and 6). This mutation also increased binding to the scrambled peptide, indicating an increase in nonspecific binding of the ApoE(130−149). Thus, D30 is an important residue for ApoE binding, but there must be other key determinants for binding ApoE(1−191)·DMPC that are missing from CR16−18.

To investigate other properties of LA3−5 that promoted interaction with ApoE, sequences of LA45 from several species were aligned, along with the corresponding repeats VLA56 in VLDLR (Figure 7a). Beyond residues conserved in all CR/LA repeats, LA4 and VLA5 showed complete conservation of a Trp at position 25 and an acidic residue at position 30 (cf. Figure 1). These residues, however, are also present in CR17, and thus, no uniquely conserved residues were found in LA4/VLA5 that might account for enhanced binding of ApoE(1−191)·DMPC. However, alignments of LA5 and VLA6 showed an additional set of highly conserved residues, E11, S17, E19, H22, W25, and K34, that were not all present in any of the CRs in LRP. While E11, S17, and W25 are quite common among all CRs in several receptors, E19 and H22 along with K34 are very rare. Previously published alignments of LA5s from various species also found H22, W25, and K34 (*52*), and residues at positions 11 and 19 were implicated in the interface of LA3 of VLDL-R with rhinovirus capsid (*53*).

To probe the importance of these residues, mutations E180A(E11A), E187A(E19A), and H190A(H22A) in LA5 were made in LA3−5. HPLC analysis of the refolded mutants showed that E180A(E11A) and E187A(E19A) mutants did not refold to a single isoform. Further, mutants E187Q(E19Q) and E187A(E19A)/K202L(K34L) also were not able to properly refold. Mutation of H190A(H22A) in LA5 had little effect on RAP binding but weakened overall ApoE(1−191)·DMPC binding (Figure 6). Similar to the G198D/P199A mutant, the H190A mutation also increased binding to the scrambled peptide,

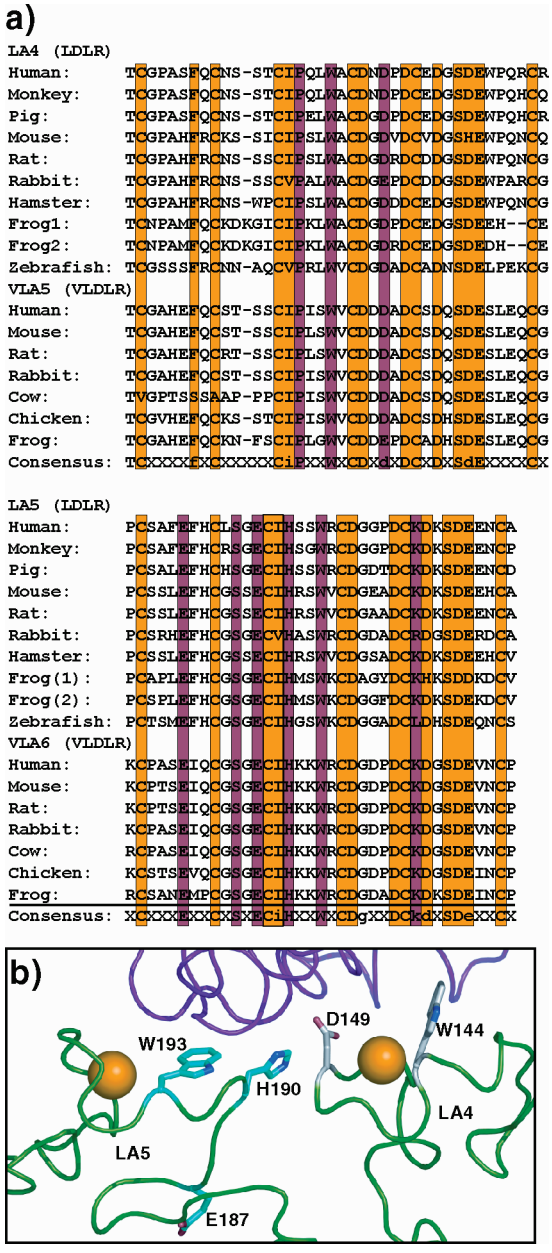

FIGURE 7: (a) Sequence alignment of LA4/VLA5 and LA5/VLA6 from various species. Consensus for these specific repeats is listed as completely conserved (upper case) and mostly conserved (lower case). Residues conserved in all complement repeats (orange) and residues specifically conserved in these repeats (purple) are highlighted. (b) Structure of LA4 (right) and LA5 (left) (from Rudenko et al. (*52*); PDB code 1N7D) with the β-propeller domain (purple), showing the specific residues implicated in binding ApoE residues 140−150 (gray) and residues implicated in binding the second site (cyan).

indicating an increase in nonspecific binding of ApoE(130−149) (Figure 5). Since we had no way of testing the importance of E187 (E19) because these mutations did not refold correctly, we instead attempted to substitute the entire β strand (residues 186−193 of LA5) into CR18 to create a possible gain-of-function CR18 variant: CR18(β2swap). This swap introduced three substitutions of residues we hypothesized are critical for binding ApoE-(1−191)·DMPC: Q19E, K22H, and F25W. To test the importance of lysine at position 34, we also introduced the A2825K(A34K) mutation into the CR16−18(β2swap) variant. Fortunately, both CR16−18(β2swap) variants refolded correctly and could interact with GST-RAP (Figure 6). These mutants

Table 2: Relative Affinities of Various CR/LA Triple Constructs from Binding Assays with GST-RAP, ApoE(1−191)·DMPC, and ApoE-(130−149)

	GST-RAP[a]	ApoE(1−191)·DMPC	ApoE (130−149)
LA3−5 WT	***	**	**
LA3−5 (D149A)	**	X	*
LA3−5 (H190A)	***	*	***
LA3−5 (GP/DA)	***	***	***
CR16−18 WT	***	X	*
CR16−18 (DDAA)	*	X	X
CR16−18 (β2s)	***	*	***
CR16−18 (β2s/AK)	***	*	***
CR173	***	X	***

[a]Symbols indicate no (X), weak (*), moderate (**), or strong (***) binding.

bound more strongly to ApoE(130−149) and more importantly, unlike wild type, could now interact with ApoE(1−191)·DMPC in a calcium-dependent manner (Figures 5 and 6). All binding data for the various constructs are summarized in Table 2. The CR16−18(β2swap) showed a specific interaction for ApoE-(1−191)·DMPC that was inhibited by both EDTA and GST-RAP just like LA3−5 (Figure 6c). As a single repeat the CR18-(β2swap) construct was also able to interact with Ub-ApoE-(130−149) with a significantly higher affinity than WT (745 ± 180 μM vs 1588 ± 338 μM).

DISCUSSION

Overall Sequence Similarity Does Not Reveal ApoE Binding Capability. Much is known about the context in which ApoE binds LDLR receptor family members, but little is known about which specific regions within the receptors bind to which specific sequences in ApoE. The dearth of information is partly due to the inability to prepare monomeric binding-active ApoE so that single specific binding events can be examined. We used sequence alignments to identify regions within the sLRPs of LRP potentially capable of binding ApoE based on sequence similarity to an ApoE binding region (LA3−5) of LDLR. We had previously shown that residues 130−149, a critical receptor binding region in ApoE, could interact with each sLRP of LRP (*32*). Despite their similarity to LA3−5, neither CR3−5 from sLRP2 nor CR25−27 from sLRP4 showed significant affinity for ApoE(130−149). In contrast, CR16−18 in sLPR3 was able to recapitulate the full binding affinity for this portion of ApoE that was observed for full sLRP3. It remains possible that other effects such as glycosylation, misfolding, or proteolytic clipping may have prevented CR3−5 and CR25−27 from binding. Regardless of this caveat, CR16−18 remained the focus of the rest of the work presented here.

Importance of the ApoE(130−149) Receptor Binding Region and Resemblance to RAP. CR16−18 was prepared in the same manner as LA3−5, and proper refolding was verified by calcium binding analyses and overlays of HSQC spectra with the individual repeats (Figure 3). Both affinity pull downs and SPR confirmed that the refolded CR16−18 could interact with ApoE(130−149) in a calcium-dependent manner and the interaction was inhibited by RAP and heparin in agreement with previous reports of other similar interactions (*32*, *41*).

Although there are subtle differences in which residues shifted in NMR titration of each CR with ApoE(130−149), the largest

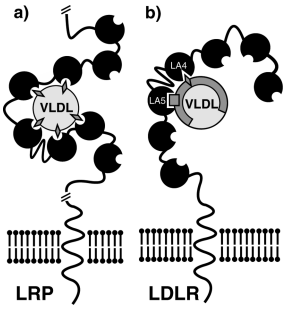

FIGURE 8: Proposed models of how LRP and LDLR might bind ApoE-containing lipoprotein particles. (a) Avidity model in which multiple copies of ApoE (gray diamonds) exposed on the particle surface combine many weak interactions with ligand binding repeats (black circles) on LRP into one strong interaction. (b) The lipoprotein-bound form of ApoE presents epitopes that are recognized by specific repeats of LDLR. In this case, LA4 is recognizing one epitope on an ApoE molecule (gray diamond), and LA5 is recognizing a different epitope (gray square).

changes were always seen for residues between the third and fifth cysteines (Figure 4a). Comparisons of ApoE(130−149) and RAPD3 titrations with single repeats indicated that the interfaces, to some extent, were similar. For both ligands the largest perturbation in CR17 and LA4 was seen in the indole of a semiconserved tryptophan at position 25 (cf. Figure 1, Supporting Information Figures 2 and 4). In addition, the amide of W25 and several nearby residues were highly shifted with both RAPD3 and ApoE(130−149), indicating that this region is involved in both interfaces.

Although ApoE(130−149) NMR titrations resulted in high uncertainty for the measured K_D, the multiple calculation methods ensured that overall trends were consistent (Table 1). The data indicate that each CR can bind Ub-ApoE(130−149) with a relatively weak affinity (high micromolar to low millimolar). CR17 had the strongest affinity for both ApoE(130−149) and RAPD3, with K_Ds similar to those seen with LA4. Both of these repeats have a Trp at position 25 and an Asp at position 30 (Figure 7). NMR titrations and pull-down assays agree that mutation of D30 ruins the interaction with RAP in agreement with previous studies (*14*). We now show that this particular Asp is also critical for the binding of ApoE(1−191)·DMPC. Both CR18 and LA3 have this critical Asp at position 30 but lack a Trp at position 25, which can explain their weaker affinity for ApoE(130−149). However, CR18 retains affinity for RAPD3 whereas LA3 has a very weak affinity for RAPD3, indicating that the RAP interaction is also dependent on residues beyond this W25/D30 pair.

In the crystal structure of RAPD3 bound to LA34, W144(W25) and D149(D30) in LA4 are at the center of the interface making contacts with lysines of RAP (*54*). CR17 probably binds RAPD3 with the same interface as seen in the crystal structure with LA4, as the largest perturbations W2778, R2777, C2781, and D2778 are at this interface. Two lysines of RAP are buried in this interface, and it is thought that lysines 143 and 146 of ApoE are similarly involved in receptor binding (*28*, *54*, *55*). Consistent with this, our ApoE(130−149)(K143/146A) double mutant showed significantly decreased affinity for CR17.

Unlike CR17 and CR18, CR16 had a much stronger affinity for ApoE(130−149) in the context of CR16−18 (730 μM vs 3.2 mM). This could be an effect of structural and dynamic perturbations from the presence of the neighboring CR17. The similar binding affinities of CR16 and CR17 when in the context of CR16−18 may lead to the speculation that only one ApoE(130−149) is binding both repeats. We think this is unlikely because the chemical shift changes observed in the single domains are identical to those observed when the domains are in the context of CR16−18. A similar enhancement was observed for LA45 binding ApoE which may also be a result of interdomain cross-talk (Guttman et al., submitted).

Avidity May Account for Much of the Observed Binding. Initial SPR experiments with CR16−18 gave K_Ds in the high nanomolar range, whereas NMR perturbation experiments with ubiquitin-fused ApoE(130−149) showed each repeat within CR16−18 binding ApoE with only high micromolar affinity. Since these affinities were not much higher than was observed for each individual repeat, the high affinity measured for CR16−18 by SPR and pull-down assay was therefore likely caused by an avidity effect in which multiple repeats simultaneously engage immobilized ApoE(130−149) molecules. This also explains the significant decrease in affinity observed upon removal of any of the three CRs.

It has previously been proposed that avidity effects, in which several interactions occur simultaneously with many copies of ApoE on LDL particle surfaces, govern the binding to the receptor (*56*). Modified ApoE·DMPC particles which contain only a single copy of active ApoE showed a 26-fold decrease in affinity for receptors compared to those with four active copies (*57*). Native lipoprotein particles can contain many copies of ApoE, so it is possible that, much like in our ApoE(130−149) studies, multiple weak interactions would account for tight binding (Figure 8). A similar avidity effect was also seen for the interaction between VLDLR repeats and human rhinovirus capsid (*53*). The observation that incorporation of ApoE(129−169) into lipoprotein particles enhances receptor-mediated particle uptake (*30*) can also be explained by this avidity mechanism.

A Distinct Binding Site on Lipid-Bound ApoE for LA5. Despite the interactions that were seen with ApoE(130−149), CR16−18 failed to show any interaction with ApoE(1−191)·DMPC (Figure 6). CR17[3] which has an even higher affinity for ApoE(130−149) was also unable to interact with lipid-bound ApoE(1−191). Since all of the constructs were correctly folded as assessed by HPLC and GST-RAP binding (Figure 6), these results strongly suggest that ApoE(1−191)·DMPC interactions involve additional features within the CR repeats beyond those required for binding ApoE(130−149). Alignments of LA45 and VLA56, thought to be the crucial repeats for ApoE binding (*41*, *43*), show high conservation of the critical W25/D30 pair in LA4 and VLA5. However, LA5, which is the most critical repeat for β-VLDL binding (*42*), does not have this Asp. Introduction of an Asp at position 30 in LA5 unexpectedly improved the binding to ApoE·DMPC (Figure 6). This Asp in LA5 is not required for ApoE·DMPC binding, but additional acidic residues may be enhancing electrostatic interactions with ApoE, which also explain the increased binding to both ApoE(130−149) and the scrambled ApoE peptide.

Since ApoE undergoes structural rearrangement upon incorporation into lipid particles (*34*, *35*, *37*), we speculated that this form of ApoE has an additional binding site which is recognized by LA5. Examination of conserved residues in LA5 and VLA6 showed a different set of conserved residues (Figure 7a). E187(E19) and H190(H22) were particularly interesting as they are very rare among these repeats but completely conserved in

LA5 and VLA6 among several species. In addition to being involved in the intramolecular interface with LDLR's β-propeller domain at endosomal pH (*52*) (Figure 7c), pull-down assays with the H190A mutant showed that the conserved H190(H22) in LA5 is also important for ApoE(1−191)·DMPC binding (Figure 6). In contrast, E187 is not positioned near the interface of LA5 with the β-propeller domain (Figure 7b). Mutation of E180(E11) and E187(E19) yielded misfolded protein, indicating that these residues are necessary for proper refolding of LA5. Previous Ala saturation mutagenesis also implicated H190(H22) in ApoE binding and could not test E187(E19) due to similar refolding problems (*58*).

When E187 (E19) along with H190 (H22) was introduced into CR18, it produced a CR16−18 variant (β2-swap) that could bind to ApoE(1−191)·DMPC in a calcium-dependent manner (Figure 6a). Lysine 202, which is semiconserved in LA5/VLA6 and is involved with the interaction with the β-propeller domain (*52*), was also introduced into this CR16−18 construct but had little effect on ApoE binding. Since CR18 has a native E11, its role was not tested; thus it is still unclear whether it is critical. This β2-swap mutation also enhanced the interaction with ApoE(130−149), as seen both by pull-down assays and NMR titrations, which can be explained by the substitution of the native Phe at position 25 with a Trp, forming the critical W25/D30 pair. The addition of this tryptophan cannot solely account for the increase in ApoE(1−191)·DMPC binding, as CR17[3] containing three copies with the critical Asp/Trp pair showed no binding to this form of ApoE (Table 2).

Taken together, these results suggest that two distinct binding events are occurring between ApoE and the LA45 repeats of LDLR (Figure 8b). The first repeat (LA4) containing the W25/D30 pair likely interacts with the 140−150 site, and the second repeat (LA5) containing an E19, H22, W25, and possibly E11 recognizes the second site that is revealed when ApoE associates with lipid particles. It is possible that helical extension of the region following residue 160 of ApoE forms this second site (*40*) and that it involves the critical R172 (*39*).

Comparison of LDLR and LRP. In the full native interaction between LDL particles and receptors, high-affinity recognition could stem from both avidity effects and lipid-induced reorganization of ApoE. Such a model might explain the observation that LDLR can clear several classes of ApoE-containing lipoproteins but LRP has only been shown to internalize ApoE-enriched β-VLDLs (*4*). LRP lacks a repeat with the critical residues in LA5 but has many repeats with the critical W25/D30 pair. Although the three-repeat construct used here was not sufficient, the larger number of repeats in the full sLRPs might form enough weak interactions to bind lipoprotein particles rich in ApoE (Figure 8). In contrast, LDLR has both types of critical repeats necessary for high-affinity binding, explaining why LA45 alone showed high affinity to ApoE(1−191)·DMPC (*41*). The observation that sLRPs 2 and 4 of LRP had higher affinities for β-VLDL (*16*) is also in agreement with this model as these two sLRPs contain more repeats with the critical W25/D30 pair (7/8 in SLRP2, 7/11 in SLRP4, only 3/10 in SLRP3). Thus lipoprotein uptake and cholesterol homeostasis may be regulated by both avidity and specific binding interactions.

ACKNOWLEDGMENT

We thank Peter J. Domaille, Ph.D., and Sangwon Lee, Ph.D., for help in setting up NMR experiments. We also thank Stephen C. Blacklow, M.D., Ph.D., for ApoE constructs.

NOTE ADDED AFTER ASAP PUBLICATION

After this paper was published online January 19, 2010, the Supporting Information was corrected. The corrected version reposted January 26, 2010.

SUPPORTING INFORMATION AVAILABLE

Additional surface plasmon resonance data supporting the binding of CR16−18 to ApoE(141−155)[2] (Figure 1), HSQC spectra showing the shifts in amide resonances during NMR titration experiments of CR16, CR17, CR18, LA3, LA4, and LA5 with Ub-ApoE(130−149) (Figure 2), HSQC spectra showing the shifts in amide resonances during NMR titration experiments of CR16−18 with Ub-ApoE(130−149) (Figure 3), and HSQC spectra showing the shifts in amide resonances during NMR titration experiments of CR17, CR18, LA3, LA4, and LA5 with Ub-RAPD3 (Figure 4). This material is available free of charge via the Internet at http://pubs.acs.org.

REFERENCES

1. Blacklow, S. C. (2007) Versatility in ligand recognition by LDL receptor family proteins: advances and frontiers. *Curr. Opin. Struct. Biol. 17*, 419–426.
2. Brown, M. S., and Goldstein, J. L. (1986) A receptor-mediated pathway for cholesterol homeostasis. *Science 232*, 34–47.
3. Hui, D. Y., Innerarity, T. L., and Mahley, R. W. (1984) Defective hepatic lipoprotein receptor binding of B-very low density lipoproteins from type 111 hyperlipoproteinemic patients: importance of apolipoprotein E. *J. Biol. Chem. 259*, 860–869.
4. Kowal, R. C., Herz, J, Goldstein, J. L., Esser, V., and Brown, M. S. (1989) Low density receptor-related protein mediates uptake of cholesteryl esters derived from apolipoprotein E-enriched lipoproteins. *Proc. Natl. Acad. Sci. U.S.A. 86*, 5810–5814.
5. Hussain, M. M., Maxfield, F. R., Más-Oliva, J., Tabas, I., Ji, Z. S., Innerarity, T. L., and Mahley, R. W. (1991) Clearance of chylomicron remnants by the low density lipoprotein receptor-related protein/alpha 2-macroglobulin receptor. *J. Biol. Chem. 266*, 13936–13940.
6. Tacken, P. J., Teusink, B., Jong, M. C., Harats, D., Havekes, L. M., van Dijk, K. W., and Hofker, M. H. (2000) LDL receptor deficiency unmasks altered VLDL triglyceride metabolism in VLDL receptor transgenic and knockout mice. *J. Lipid Res. 41*, 2055–2062.
7. Takahashi, S., Kawarabayasi, Y., Nakai, T., Sakai, J., and Yamamoto, T. (1992) Rabbit very low density lipoprotein receptor: a low density lipoprotein receptor-like protein with distinct ligand specificity. *Proc. Natl. Acad. Sci. U.S.A. 89*, 9252–9256.
8. Herz, J., and Strickland, D. K. (2001) LRP: a multifunctional scavenger and signaling receptor. *J. Clin. Invest. 108*, 779–784.
9. Willnow, T. E., Moehring, J. M., Inocencio, N. M., Moehring, T. J., and Herz, J. (1996) The low-density-lipoprotein receptor-related protein (LRP) is processed by furin in vivo and in vitro. *Biochem. J. 313*, 71–76.
10. Willnow, T. E., Armstrong, S. A., Hammer, R. E., and Herz, J. (1995) Functional expression of low density lipoprotein receptor-related protein is controlled by receptor-associated protein in vivo. *Proc. Natl. Acad. Sci. U.S.A. 92*, 4537–4541.
11. Bu, G., and Rennke, S. (1996) Receptor-associated protein is a folding chaperone for low density lipoprotein receptor-related protein. *J. Biol. Chem. 271*, 22218–22224.
12. Herz, J., Goldstein, J. L., Strickland, D. K., Ho, Y. K., and Brown, M. S. (1991) 39-kDa protein modulates binding of ligands to low density lipoprotein receptor-related protein/alpha 2-macroglobulin receptor. *J. Biol. Chem. 266*, 21232–21238.
13. Andersen, O. M., Schwarz, F. P., Eisenstein, E., Jacobsen, C., Moestrup, S. K., Etzerodt, M., and Thøgersen, H. C. (2001) Dominant thermodynamic role of the third independent receptor binding site in the receptor-associated protein RAP. *Biochem. J. 40*, 15408–15417.
14. Andersen, O. M., Christensen, L. L., Christensen, P. A., Sørensen, E. S., Jacobsen, C., Moestrup, S. K., Etzerodt, M., and Thogersen, H. C. (2000) Identification of the minimal functional unit in the low density lipoprotein receptor-related protein for binding the receptor-associated protein (RAP). A conserved acidic residue in the complement-type repeats is important for recognition of RAP. *J. Biol. Chem. 275*, 21017–21024.

15. Willnow, T. E., Orth, K., and Herz, J. (1994) Molecular dissection of ligand binding sites on the low density lipoprotein receptor-related protein. *J. Biol. Chem. 269*, 15827–15832.
16. Neels, J. G., van den Berg, B. M. M., Lookene, A., Olivecrona, G., Pannekoek, H., and van Zonneveld, A. J. (1999) The second and fourth cluster of class A cysteine-rich repeats of the low density lipoprotein receptor-related protein share ligand binding properties. *J. Biol. Chem. 274*, 31305–31311.
17. Horn, I. R., van den Berg, B. M., van der Meijden, P. Z., Pannekoek, H., and van Zonneveld, A. J. (1997) Molecular analysis of ligand binding to the second cluster of complement-type repeats of the low density lipoprotein receptor-related protein. Evidence for an allosteric component in receptor-associated protein-mediated inhibition of ligand binding. *J. Biol. Chem. 272*, 13608–13613.
18. Croy, J. E., Shin, W. D., Knauer, M. F., Knauer, D. J., and Komives, E. A. (2003) All three LDL receptor homology regions of the LDL receptor-related protein (LRP) bind multiple ligands. *Biochemistry 42*, 13049–13057.
19. Beisiegel, U., Weber, W., Ihrke, G., Herz, J., and Stanley, K. K. (1989) The LDL-receptor-related protein, LRP, is an apolipoprotein E-binding protein. *Nature 341*, 162–164.
20. Mokuno, H., Yamada, N., Shimano, H., Ishibashi, S., Mori, N., Takahashi, K., Oka, T., Yoon, T. H., and Takaku, F. (1991) The enhanced cellular uptake of very-low-density lipoprotein enriched in apolipoprotein E. *Biochim. Biophys. Acta 1082*, 63–70.
21. Blacklow, S. C., and Kim, P. S. (1996) Protein folding and calcium binding defects arising from familial hypercholesterolemia mutations of the LDL receptor. *Nat. Struct. Biol. 3*, 758–762.
22. Rudenko, G., and Deisenhofer, J. (2003) The low-density lipoprotein receptor: ligands, debates and lore. *Curr. Opin. Struct. Biol. 13*, 683–689.
23. Huang, W., Dolmer, K., and Gettins, P. G. (1999) NMR solution structure of complement-like repeat CR8 from the low density lipoprotein receptor-related protein. *J. Biol. Chem. 274*, 14130–14136.
24. Rall, S. C. J., Weisgraber, K. H., Innerarity, T. L., and Mahley, R. W. (1982) Structural basis for receptor binding heterogeneity of apolipoprotein E from type III hyperlipoproteinemic subjects. *Proc. Natl. Acad. Sci. U.S.A. 79*, 4696–4700.
25. Innerarity, T. L., Friedlander, E. J., Rall, S. C. J., Weisgraber, K. H., and Mahley, R. W. (1983) The receptor binding domain of human apolipoprotein E. Binding of apolipoprotein E fragments. *J. Biol. Chem. 258*, 12341–12347.
26. Weisgraber, K. L., Innerarity, T. L., Harder, K. J., Mahley, R. W., Milne, R. W., Marcel, Y. L., and Sparrow, J. T. (1983) The receptor binding domain of human apolipoprotein E. *J. Biol. Chem. 258*, 12348–12354.
27. Lalazar, A., Weisgraber, K. H., Rall, S. C. J., Gilad, H., Innerarity, T. L., Levanon, A. Z., Boyles, J. K., Amit, B., Gorecki, M., Mahley, R. W., and Vogel, T. (1988) Site-specific mutagenesis of human apolipoprotein E. Receptor binding activity of variants with single amino acids substitutions. *J. Biol. Chem. 263*, 3542–3545.
28. Zaiou, M., Arnold, K. S., Newhouse, Y. M., Innerarity, T. L., Weisgraber, K. H., Segall, M. L., Phillips, M. C., and Lund-Katz, S. (2000) Apolipoprotein E; low density lipoprotein receptor interaction. Influences of basic residue and amphipathic alpha-helix organization in the ligand. *J. Lipid Res. 41*, 1087–1095.
29. Kiss, R. S., Weers, P. M., Narayanaswami, V., Cohen, J., Kay, C. M., and Ryan, R. O. (2003) Structure-guided protein engineering modulates helix bundle exchangeable apolipoprotein properties. *J. Biol. Chem. 278*, 21952–21959.
30. Mims, M. P., Darnule, A. T., Tovar, R. W., Pownall, H. J., Sparrow, D. A., Sparrow, J. T., Via, D. P., and Smith, L. C. (1994) A nonexchangeable apolipoprotein E peptide that mediates binding to the low density lipoprotein receptor. *J. Biol. Chem. 269*, 20539–20547.
31. Datta, G., Garber, D. W., Chung, B. H., Chaddha, M., Dashti, N., Bradley, W. A., Gianturco, S. H., and Anantharamaiah, G. M. (2001) Cationic domain 141−150 of apoE covalently linked to a class A amphipathic helix enhances atherogenic lipoprotein metabolism in vitro and in vivo. *J. Lipid Res. 42*, 959–966.
32. Croy, J. E., Brandon, T., and Komives, E. A. (2004) Two apolipoprotein E mimetic peptides, apoE(130−149) and apoE(141−155)2, bind to LRP1. *Biochemistry 43*, 7328–7335.
33. Wilson, C., Wardell, M. R., Weisgraber, K. H., Mahley, R. W., and Agard, D. A. (1991) Three-dimensional structure of the LDL receptor-binding domain of human apolipoprotein E. *Science 252*, 1817–1822.
34. Fisher, C. A., and Ryan, R. O. (1999) Lipid binding-induced conformational changes in the N-terminal domain of human apolipoprotein E. *J. Lipid Res. 40*, 93–99.
35. Peters-Libeu, C. A., Newhouse, Y., Hatters, D. M., and Weisgraber, K. H. (2006) Model of biologically active apolipoprotein E bound to dipalmitoylphosphatidylcholine. *J. Biol. Chem. 281*, 1073–1079.
36. Peters-Libeu, C. A., Newhouse, Y., Hall, S. C., Witkowska, H. E., and Weisgraber, K. H. (2007) Apolipoprotein E·dipalmitoylphosphatidylcholine particles are ellipsoidal in solution. *J. Lipid Res. 48*, 1035–1044.
37. Lund-Katz, S., Zaiou, M., Wehrli, S., Dhanasekaran, P., Baldwin, F., Weisgraber, K. H., and Phillips, M. C. (2000) Effects of lipid interaction on the lysine microenvironments in apolipoprotein E. *J. Biol. Chem. 275*, 34459–34464.
38. Lalazar, A., and Mahley, R. W. (1989) Human apolipoprotein E. Receptor binding activity of truncated variants with carboxyl-terminal deletions. *J. Biol. Chem. 264*, 8447–8450.
39. Morrow, J. A., Arnold, K. S., Dong, J., Balesta, M. E., and Innerarity, T. L. (2000) Effect of arginine 172 on the binding of apolipoprotein E to the low density lipoprotein receptor. *J. Biol. Chem. 275*, 2576–2580.
40. Gupta, V., Narayanaswami, V., Budamagunta, M. S., Yamamato, T., Voss, J. C., and Ryan, R. O. (2006) Lipid-induced extension of apolipoprotein E helix 4 correlates with low density lipoprotein receptor binding ability. *J. Biol. Chem. 281*, 39294–39299.
41. Fisher, C., Abdul-Aziz, D., and Blacklow, S. C. (2004) A two-module region of the low-density lipoprotein receptor sufficient for formation of complexes with apolipoprotein E ligands. *Biochem. J. 43*, 1037–1044.
42. Russell, D. W., Brown, M. S., and Goldstein, J. L. (1989) Different combinations of cysteine-rich repeats mediate binding of low density lipoprotein receptor to two different proteins. *J. Biol. Chem. 264*, 21682–21688.
43. Ruiz, J., Kouiavskaia, D., Migliorini, M., Robinson, S., Saenko, E. L., Gorlatova, N., Li, D., Lawrence, D., Hyman, B. T., Weisgraber, K. H., and Strickland, D. K. (2005) The apoE isoform binding properties of the VLDL receptor reveal marked differences from LRP and the LDL receptor. *J. Lipid Res. 46*, 1721–1731.
44. Nicholas, K. B., Nicholas, H. B., Jr., and Deerfield, D. W., II. (1997) GeneDoc: Analysis and visualization of genetic variation. *EMBnet. NEWS* 4, 14.
45. White, C. E., Hunter, M. J., Meininger, D. P., White, L. R., and Komives, E. A. (1995) Large-scale expression, purification and characterization of small fragments of thrombomodulin: the roles of the sixth domain and of methionine 388. *Protein Eng. 8*, 1177–1187.
46. Fass, D., Blacklow, S., Kim, P. S., and Berger, J. M. (1997) Molecular basis of familial hypercholesterolaemia from structure of LDL receptor module. *Nature 388*, 691–693.
47. Clackson, T., Detlef, G., and Jones, P. (1991) PCR, a Practical Approach (McPherson, M., Quirke, P., and Taylor, G., Eds.) p 202, IRL Press, Oxford.
48. Jez, M., J., Ferrer, J., Bowman, M., E., Dixon, R., A., and Noel, J., P. (2000) Dissection of malonyl-coenzyme A decarboxylation from polyketide formation in the reaction mechanism of a plant polyketide synthase. *Biochemistry 39*, 890–902.
49. Hoffman, R. M. B., Li, M. X., and Sykes, B. D. (2005) The binding of W7, an inhibitor of striated muscle contraction, to cardiac troponin C. *Biochemistry 44*, 15750–15759.
50. Andersen, O. M., Vorum, H., Honoré, B., and Thøgersen, H. C. (2003) Ca^{2+} binding to complement-type repeat domains 5 and 6 from the low-density lipoprotein receptor-related protein. *BMC Biochem. 4*, 7.
51. Simonovic, M., Dolmer, K., Huang, W., Strickland, D. K., Volz, K., and Gettins, P. G. W. (2001) Calcuim coordination and pH dependence of the calcium affinity of ligand-binding repeat CR7 from the LRP. Comparision with related domains from the LRP and the LDL receptor. *Biochemistry 40*, 15127–15134.
52. Rudenko, G., Henry, L., Henderson, K., Ichtchenko, K., Brown, M. S., Goldstein, J. L., and Deisenhofer, J. (2002) Structure of the LDL receptor extracellular domain at endosomal pH. *Science 298*, 2353–2358.
53. Verdaguer, N., Fita, I., Reithmayer, M., Moser, R., and Blaas, D. (2004) X-ray structure of a minor group human rhinovirus bound to a fragment of its cellular receptor protein. *Nat. Struct. Mol. Biol. 11*, 429–434.
54. Fisher, C., Beglova, N., and Blacklow, S. C. (2006) Structure of an LDLR-RAP complex reveals a general mode for ligand recognition by lipoprotein receptors. *Mol. Cell 22*, 277–283.
55. Prévost, M., and Raussens, V. (2004) Apolipoprotein E-low density lipoprotein receptor binding: study of protein-protein interaction in rationally selected docked complexes. *Proteins 55*, 874–884.
56. Mahley, R. W., Innerarity, T. L., Rall, S. C., and Weisgraber, K. H. (1984) Plasma lipoproteins: apolipoprotein structure and function. *J. Lipid Res. 25*, 1277–1294.
57. Pitas, R. E., Innerarity, T. L., and Mahley, R. W. (1980) Cell surface receptor binding of phospholipid·protein complexes containing different ratios of receptor-active and -inactive E apoprotein. *J. Biol. Chem. 255*, 5454–5460.
58. Abdul-Aziz, D., Fisher, C., Beglova, N., and Blacklow, S. C. (2005) Folding and binding integrity of variants of a prototype ligand-binding module from the LDL receptor possessing multiple alanine substitutions. *Biochem. J. 44*, 5075–5085.